

Article

Surface Properties of Aqueous Dispersions of Bovine Serum Albumin Fibrils

Alexander Akentiev ¹, Shi-Yow Lin ², Giuseppe Loglio ³, Reinhard Miller ⁴ and Boris Noskov ^{1,*}

¹ Department of Colloid Chemistry, St. Petersburg State University, Universitetsky pr. 26, 198504 St. Petersburg, Russia; a.akentiev@spbu.ru

² Chemical Engineering Department, National Taiwan University of Science and Technology, Taipei 106, Taiwan; sylin@mail.ntust.edu.tw

³ Institute of Condensed Matter Chemistry and Technologies for Energy, 16149 Genoa, Italy; giuseppe.loglio@ge.icmate.cnr.it

⁴ Institute for Condensed Matter Physics, Technical University Darmstadt, 64289 Darmstadt, Germany; miller@fkp.tu-darmstadt.de

* Correspondence: borisanno@rambler.ru; Tel.: +7-8124284093

Abstract: The surface properties of aqueous dispersions of worm-like fibril aggregates of bovine serum albumin (BSA) differ from those of the adsorption layers of the native protein. The dispersions of BSA fibrils are characterized by slower changes of the surface tension and dynamic surface elasticity and also have different steady-state values of the surface properties. The fourfold compression of the adsorption layer of BSA fibrils leads to noticeably higher surface pressures than those of a compressed layer of the native protein, indicating the formation of a more rigid layer structure in the former case. The spreading of BSA fibrils onto a liquid surface from a concentrated dispersion reduces the effect of surface-active admixtures on the layer properties. The dependencies of the dynamic surface elasticity on surface pressure almost coincide for the spread layers of fibrils and the native protein in the range of low surface pressures, but only the spreading of the native protein can lead to surface pressures higher than 4 mN/m. This distinction is presumably caused by the formation of stable clusters of BSA fibrils at the interface and their slow propagation along the liquid surface.

Keywords: bovine serum albumin fibrils; adsorbed layers; spread layers; surface dilational viscoelasticity; atomic force microscopy



Citation: Akentiev, A.; Lin, S.-Y.; Loglio, G.; Miller, R.; Noskov, B. Surface Properties of Aqueous Dispersions of Bovine Serum Albumin Fibrils. *Colloids Interfaces* **2023**, *7*, 59. <https://doi.org/10.3390/colloids7030059>

Academic Editor: Emilia Nowak

Received: 29 June 2023

Revised: 24 August 2023

Accepted: 8 September 2023

Published: 14 September 2023



Copyright: © 2023 by the authors. Licensee MDPI, Basel, Switzerland. This article is an open access article distributed under the terms and conditions of the Creative Commons Attribution (CC BY) license (<https://creativecommons.org/licenses/by/4.0/>).

1. Introduction

The formation of amyloid fibrils in the human body can result in neurodegenerative diseases such as Alzheimer's, Parkinson's disease, and type 2 diabetes [1–5]. At the same time, some fibrils can play an important role in vital processes in bacteria, animals, and humans. For example, they are responsible for the strength and elasticity of the spider web and are formed in human melanosomes, accelerating melanin formation [6,7]. Due to their unique properties, amyloid fibrils have recently found various applications in biotechnology and can be used to produce drug delivery systems, photovoltaic cells, photoluminescent tags, biosensors, and scaffolds for cell cultures [8–12].

A growing area of applications of protein fibrils is the stabilization of foams and emulsions [13–17]. Many proteins and their aggregates have a high surface activity [18–20] and can be used to stabilize dispersion systems in pharmaceutical and food industries, where the use of inorganic stabilizers is very limited. At the same time, while high concentrations of native proteins are often required for these purposes, the application of fibrils reduces the total protein concentration and thereby decreases the cost of the products. The information on properties of the adsorption layers of protein fibrils is rather limited, and most publications are devoted to the layers of aggregates of three model proteins—beta-lactoglobulin (BLG), ovalbumin, and lysozyme [18,19,21–24]. The adsorption and spread layers of fibrils

of other proteins, for example, of bovine serum albumin (BSA), practically have not been studied yet to the best of our knowledge.

BSA is a carrier of various substances in the circulatory blood system and is contained in large quantities in blood plasma. The formation of nano- and microparticles on the basis of this protein can find various applications in the pharmaceutical industry [25,26]. Similar to some other proteins, BSA is able to form curly worm-like aggregates that differ from conventional fibrils not only in shape and size but also in their properties [27]. The main distinguishing feature of such worm-like aggregates is not only a strong skeleton of β -sheets but also a large number of α -helices, which can prevent the formation of high-order structures. Although many publications have appeared recently on the methods of preparation, morphology, and bulk properties of BSA fibril dispersions, as far as we know, there is no information on the surface properties of these systems [27–36]. The present study is devoted to the determination of the properties of the layers of BSA fibrils at the air–water interface.

2. Materials and Methods

2.1. Materials

A relatively concentrated solution (20 mM) of BSA (Sigma–Aldrich, Steinheim, Germany, MW 66,000 kDa) in Tris-HCl buffer (pH 7.4) was purified by dialysis over four days using a cellulose membrane (Sigma–Aldrich, Steinheim, Germany). After the dialysis, the solution was centrifuged at $15,500 \times g$ for 30 min and then filtered with the aim to remove insoluble particles. After that, the protein solution was diluted to a final concentration of about 2.5 wt.% with the TrisHCl buffer. The amyloid fibrils were prepared according to the method of Holm et al. [27]. The BSA solution was incubated in a thermostat for 96 h at a temperature of 70 °C without stirring. Finally, the obtained fibril dispersion was cooled fast in ice water. The dispersion presumably contained not only fibrils but some non-reacted proteins and peptides of low molecular weight and high surface activity [21,37,38]. The purification of the fibril dispersion from by-products was carried out by centrifugation for an hour ($55,000 \times g$) at a temperature of 4 °C. After that, the supernatant was carefully removed, and the precipitate was dissolved in the TrisHCl buffer solution or water at pH 2 and placed in a refrigerator without shaking. A cloudy viscous homogeneous solution was formed there in a few days using the two solvents. Note that a strong shaking of the solution can lead to the destruction of the formed fibrils. Therefore, the preservation of the fibril size was controlled by atomic force microscopy (AFM).

All the solutions were prepared in triply distilled water. A TrismaBase (Sigma–Aldrich) buffer solution with a concentration of 20 mM was adjusted to the required pH using small additions of HCl (Vecton, Russia). Sodium chloride (Vecton, Russia) was calcined for 8 h at a temperature of 700 °C to remove organic impurities. The dispersions of a required fibril concentration were prepared 24 h before the measurements in order to obtain a completely homogeneous dispersion and stored in a refrigerator at 4 °C. The fibril concentration in the dispersions was determined gravimetrically.

2.2. Methods

BSA fibrils were spread by a micro-syringe onto a cleaned surface of the subphase using a glass plate. The cleaning of the liquid surface before the beginning of measurements was carried out using a Pasteur pipette and a pump.

The dynamic surface elasticity was determined by the oscillating barrier method using the ISR instrument (KSVNima, Helsinki, Finland) as described earlier [39,40]. The measurements were carried out in a PTFE Langmuir trough of 7.5 cm wide and 0.5 cm deep, equipped with two PTFE barriers located at a distance of 17 cm from each other. The oscillations of the surface tension occurred as a result of a sinusoidal reciprocating motion of the barriers with a frequency of 30 mHz and an amplitude of 2% and were measured by the Wilhelmy plate method. The platinum plate was located in the middle of the trough between the barriers and oriented parallel to them. The complex dynamic surface elasticity

ε was defined as the ratio of the complex amplitudes of oscillations of the surface tension γ and surface area A :

$$\varepsilon = \varepsilon_{Re} + \varepsilon_{Im} = A \frac{\delta\gamma}{\delta A} \quad (1)$$

The imaginary part of the dynamic surface elasticity ε_{Im} did not exceed 5% of the real part ε_{Re} in all the measurements and is not presented below. The accuracy of measurements of ε_{Re} and the elasticity modulus ε is approximately $\pm 3\%$.

The shape of fibrils and the micromorphology of the fibril layers were determined by AFM using a NTEGRA Spectra instrument (NT-MDT, Russia) in a semi-contact mode. A drop of the dispersion was placed onto the surface of a freshly cleaned mica plate, dried for a few days, and the surface was scanned after that to determine the fibril shape and size. The morphology of the layer was evaluated after its transfer from the liquid surface onto a mica plate by the Langmuir–Schaeffer method.

The macromorphology of fibril layers on the liquid surface was determined in situ by Brewster angle microscopy using a BAM1 instrument (Nanofilm Technology, Geottingen, Germany).

All the measurements of surface properties were carried out at a temperature of 23 °C.

3. Results and Discussions

Figure 1 shows the AFM images of BSA fibrils for dispersions in water before and after centrifugation. Similar AFM images were obtained for dispersions in the TrisHCl buffer (Figure S1). Note that TrisHCl contaminates the fibril layer on the mica surface, resulting in less informative images.

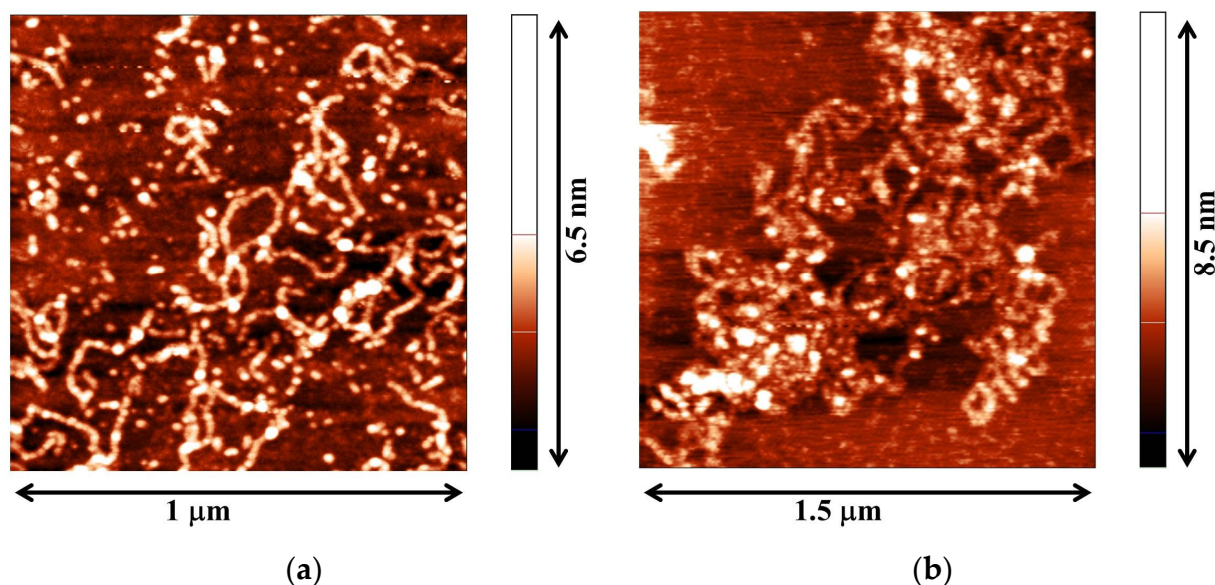


Figure 1. AFM images of BSA fibrils before (a) and after (b) purification.

One can see a large number of curly worm-like BSA fibrils similar to the fibrils obtained by Holm et al. [27]. These aggregates differ significantly from the fibrils of BLG and lysozyme [21], and thereby, it is possible to expect different properties of their dispersions. In addition to the fibrils, there are also a large number of small aggregates in Figure 1a. The purification by centrifugation decreases the number of these aggregates (Figure 1b) and also the concentration of impurities of high surface activity, as shown below.

Figure 2 shows the kinetic dependences of surface tension and dynamic surface elasticity of fibril dispersions (before and after purification) and native BSA solutions with a concentration of 0.015 g/L in 0.1 M NaCl at pH 5.5. The dispersions of fibrils after purification are characterized by an induction period of about one hour, after which the surface tension slowly drops to 61.5 mN/m, and the dynamic surface elasticity increases up to

44 mN/m. Moreover, the steady-state surface elasticity is reached faster than the steady-state surface tension. The changes of the surface properties are faster for dispersions of unpurified fibrils, presumably due to the impurities of high surface activity. The deceleration of these changes after purification indicates an effective purification procedure.

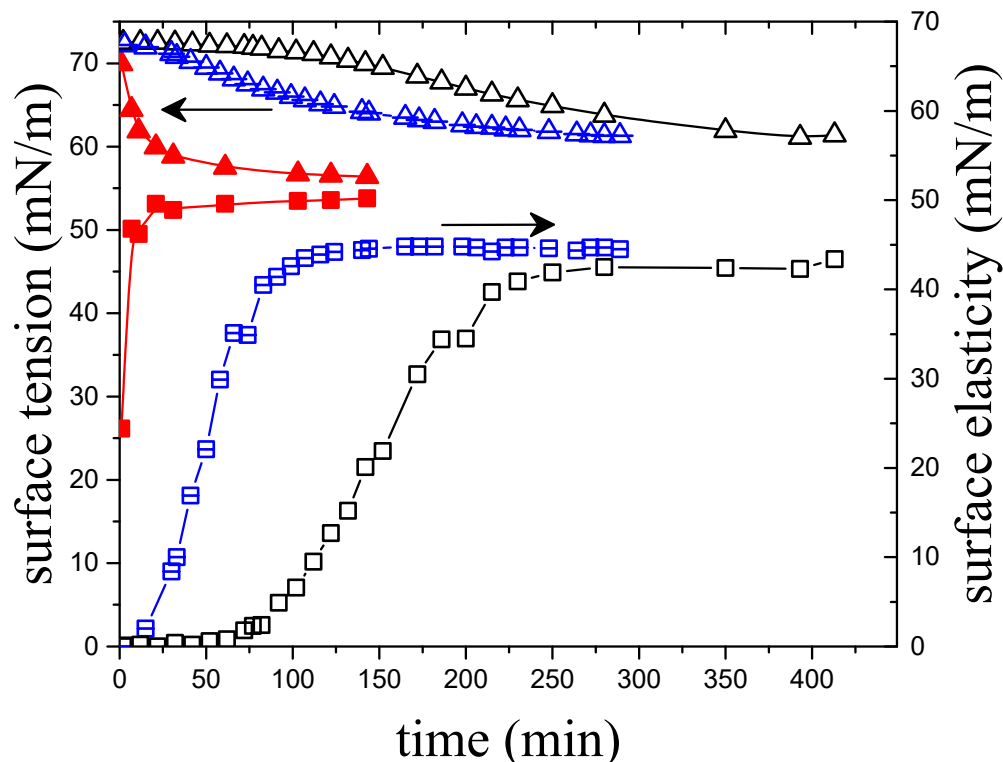


Figure 2. Kinetic dependences of the surface tension (triangles) and dynamic surface elasticity (squares) of native BSA solutions (red filled symbols), dispersions of unpurified BSA fibrils (blue symbols with a dash), and of purified BSA fibrils (black empty symbols). The protein concentration in 0.1 M NaCl is 0.015 g/L. The arrows relate the data to the corresponding axes.

The kinetic dependences of the surface properties of native protein solutions at a concentration of 0.015 g/L do not show an induction period and are similar to previous results [41]. The steady-state values of the surface properties are reached within approximately 30 min after surface formation. The slower changes in the surface properties of the dispersions of BSA fibril aggregates can be associated with larger kinetic units in this case and, consequently, with a decrease in the diffusion coefficient.

The steady-state values of the surface properties of native BSA solutions and fibril dispersions do not coincide, and the observed differences are beyond experimental errors (1 and 3%, respectively).

At the same time, the dependences of the dynamic surface elasticity on surface pressure almost coincide with a wide range of surface pressures (Figure 3). When the surface pressure of fibril dispersions reaches about 12 mN/m, the surface properties almost do not change after that, while in the case of native BSA solutions, the surface pressure increases up to 17 mN/m. The spontaneous adsorption can result in higher surface pressures for native protein molecules than for fibrils due to the peculiarities of the layer structures.

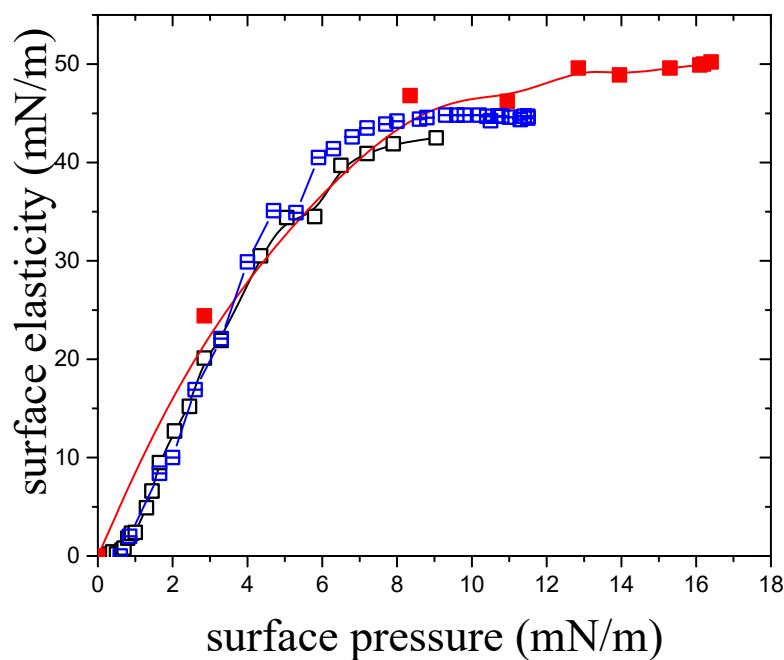


Figure 3. Dependences of the dynamic surface elasticity on surface pressure of native BSA solutions (red filled squares), dispersions of unpurified fibrils (blue squares with a dash), and purified fibrils (black empty squares).

Fourfold compression of the adsorption layers of the native protein and its fibril aggregates at a rate of 5 mm/min leads to different surface pressure isotherms. Although the results in Figure 4 depend in both cases on the compression rate, the obtained dynamic data presumably indicate the formation of a relatively rigid fibril network at the water surface under compression. At the same time, the native protein molecules can go easier to the subphase, thereby leading to lower surface pressures.

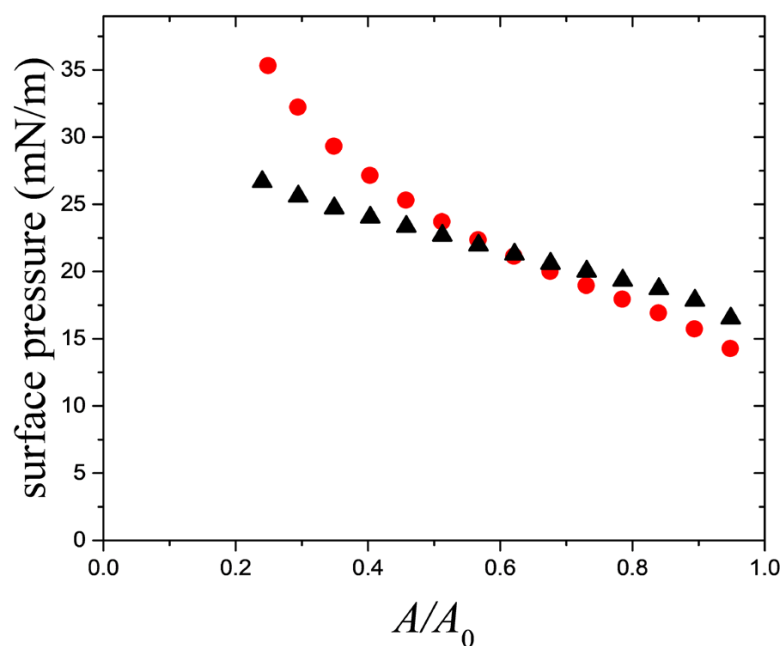


Figure 4. Compression isotherms of the adsorption layers of native BSA (red circles) and fibrils (black triangles). The concentration of native BSA and BSA fibrils is 0.015 g/l. A_0 —the initial surface area (A —is the area between barriers at the given moment, cf. Equation (1)).

The AFM images of adsorption layers of BSA fibril aggregates on the surface of a 0.1 M sodium chloride solution, which were transferred onto the mica surface, are shown in Figure 5. The images of the layers in 12 h after the surface formation before surface compression can be approximately divided into two groups (Figure 5a,b). In the first case, one can observe a dense layer with a large number of intertwined fibrils (Figure 5a), while in the second case (Figure 5b), there are separate branched clusters of fibril aggregates. The two types of AFM images have also been observed earlier for adsorption layers of lysozyme fibrils [21]. The fourfold surface compression leads to a thicker and denser layer without a great number of large aggregates (Figure 5c).

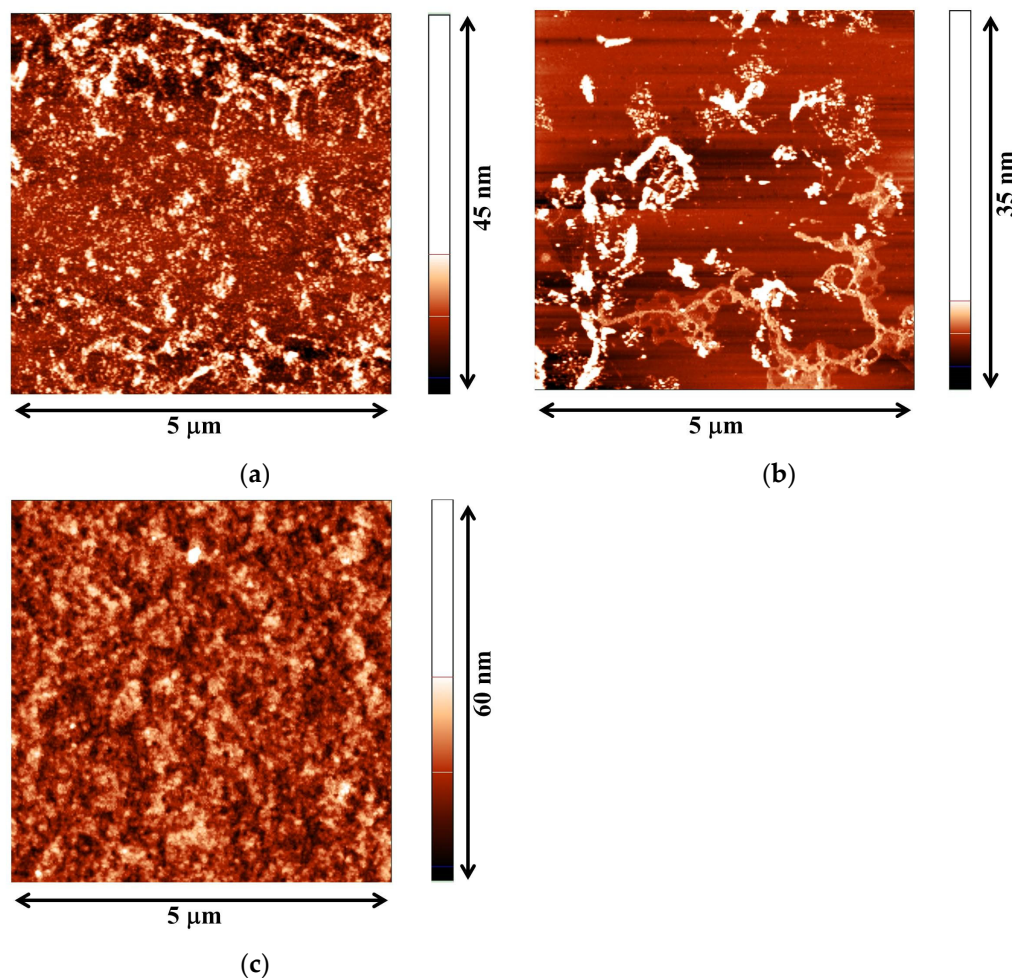


Figure 5. AFM images of the adsorption layers of BSA fibrils transferred from the surface of a 0.1 M NaCl aqueous solution onto the mica surface: (a,b) before compression at the surface pressure of 10 mN/m; (c) after fourfold compression at a surface pressure of 38 mN/m.

The kinetic dependencies of the surface properties of BSA fibril dispersions depend strongly on the solution's ionic strength (Figure 6). The rate of change of the surface properties increases with the ionic strength at the approach to steady-state values due to a decrease in the electrostatic adsorption barrier. The strong influence of the increase of the ionic strength on surface properties can also be connected with a decrease in the sub-microbubble concentration in the surface layer [42].

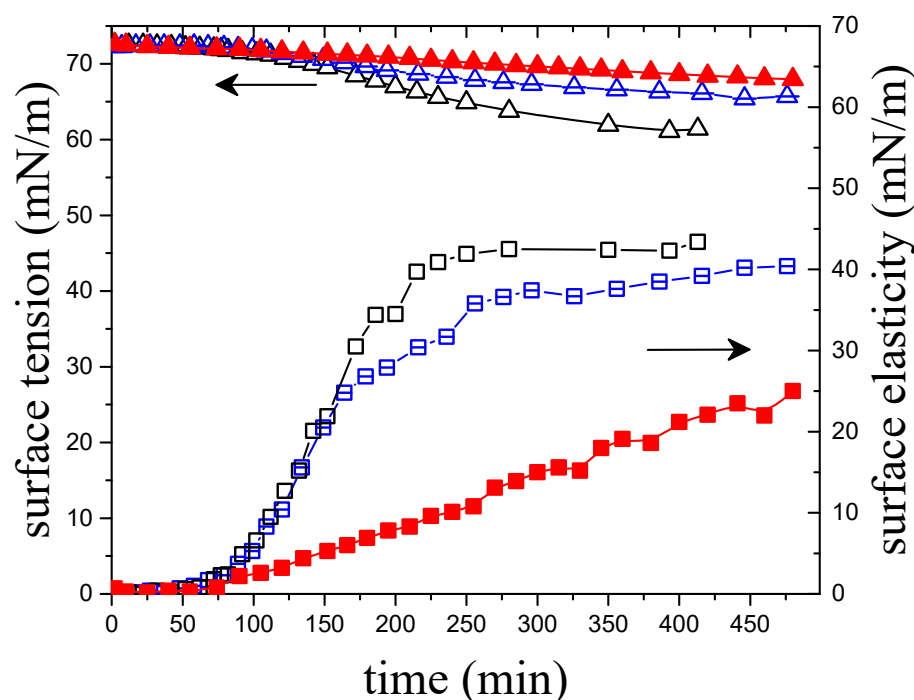


Figure 6. Kinetic dependences of the surface tension (triangles) and dynamic surface elasticity (squares) of the dispersions of BSA fibrils in water (red filled symbols), in a TrisHCl buffer (blue symbols with a dash), and 0.1 M NaCl (black empty symbols). The arrows relate the data to the corresponding axes.

The influence of impurities on the properties of spread layers is less than on the properties of the adsorption layers [21]. In adsorption layers, the local impurity concentration is relatively high due to its higher surface activity, while in spread layers, the concentrations of impurities and fibrils almost coincide with the values in the bulk phase, and thereby, the impurity concentration is much lower than in the former case.

The surface pressure increases to 4 mN/m and the surface elasticity up to 38 mN/m if the fibril dispersion with a concentration of 0.4 g/L is spread drop by drop onto the surface of a 0.1 M aqueous NaCl solution (Figure 7). The further addition of the dispersion does not lead to noticeable changes in the surface properties. Therefore, the fibril spreading along the surface leads to lower surface pressures than the adsorption from the fibril dispersion (Figure 3). This distinction may be due to the strong influence of impurities in the case of adsorption and/or due to the formation of dense and stable clusters of fibrils in the region where the dispersion drops touch the surface. A similar effect of the formation of stable clusters of lysozyme microgel particles at the interface was observed in the case of spreading their dispersion onto the water surface [43].

Further changes in the surface concentration of fibrils in spread layers were carried out by stepwise layer compressions. At relatively high surface concentrations, the compression of the layer led to a noticeable increase in the surface pressure with slow changes in the dynamic surface elasticity (Figure 7). Only at surface pressures above 18 mN/m can one see a sharp increase in the surface elasticity. In this case, when the compression stopped, the surface pressure dropped much stronger than in the range of lower surface pressures (<18 mN/m, Figure S2). Note that the successive compressions of the native protein layers led only to a slight increase of the surface properties with a much weaker relaxation when the compression was stopped.

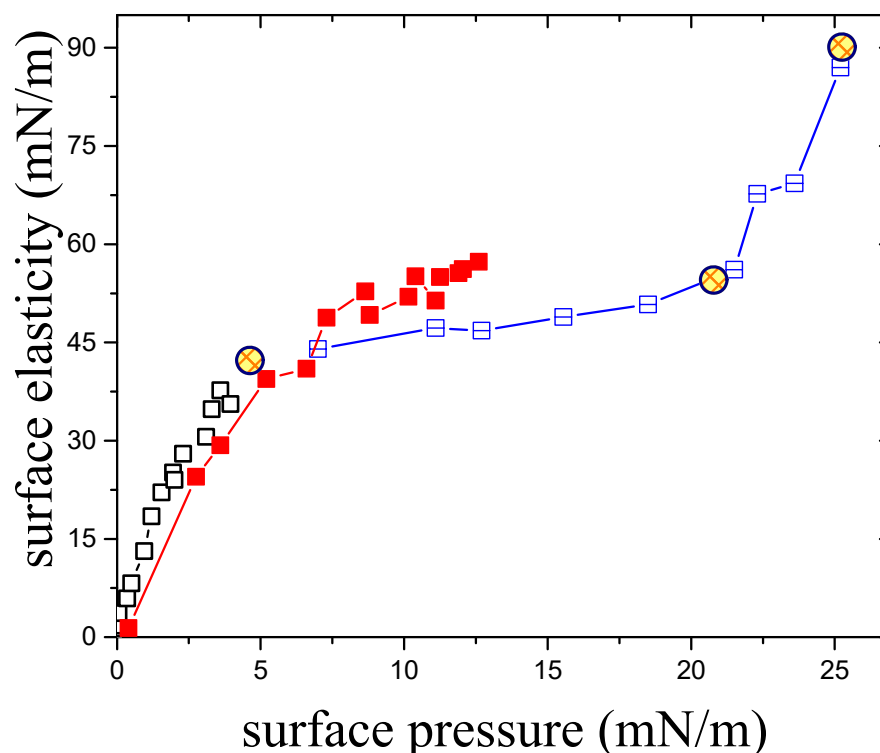


Figure 7. Dependencies of the dynamic surface elasticity on surface pressure for spread layers of native BSA (red filled squares) and BSA fibrils, which were obtained by sequential additions of small portions of the dispersion (black empty squares) and by compression of a spread layer (blue squares with a dash). Circles mark the surface properties corresponding to the transfer of the layer onto a mica plate.

The results for spread layers of BSA fibrils give a possibility to trace the changes in the layer structure. When the dispersion is spread onto the liquid surface, the AFM shows that the fibril layer has a large number of holes (Figure 8a,b). It is characterized by relatively low surface pressures, 0–4 mN/m, and a noticeable surface elasticity of up to ~38 mN/m. The further addition of fibrils at surface pressures of about 4 mN/m does not lead to their noticeable spreading along the surface. The subsequent layer compression increases the surface pressure due to the increase of the surface concentration of hydrophobic groups but leads only to a slight increase of the surface elasticity, indicating the preservation of a relatively loose layer structure with some holes. When the surface pressure reaches about 18 mN/m, the holes almost disappear (Figure 8c,d), the layer structure becomes more rigid, and the elasticity starts to increase abruptly. At the fourfold compression, the AFM images show a dense layer of fibrils without holes but with some folds (Figure 8e,f), and the dynamic surface elasticity reaches high values (~90 mN/m). When the surface is expanded, the holes appear again, leading to a decrease of the surface pressure and the dynamic surface elasticity (Figures S2 and S3a,b).

The BAM images do not show noticeable changes in the macroscopic morphology of the layer, which preserves its homogeneity upon compression (Figure S4a,b). A slight disturbance of the surface by a thin rod leads to a hardly noticeable trail, but it disappears completely within a few minutes, indicating a liquid-like nature of the fibril layer (Figure S4c,d).

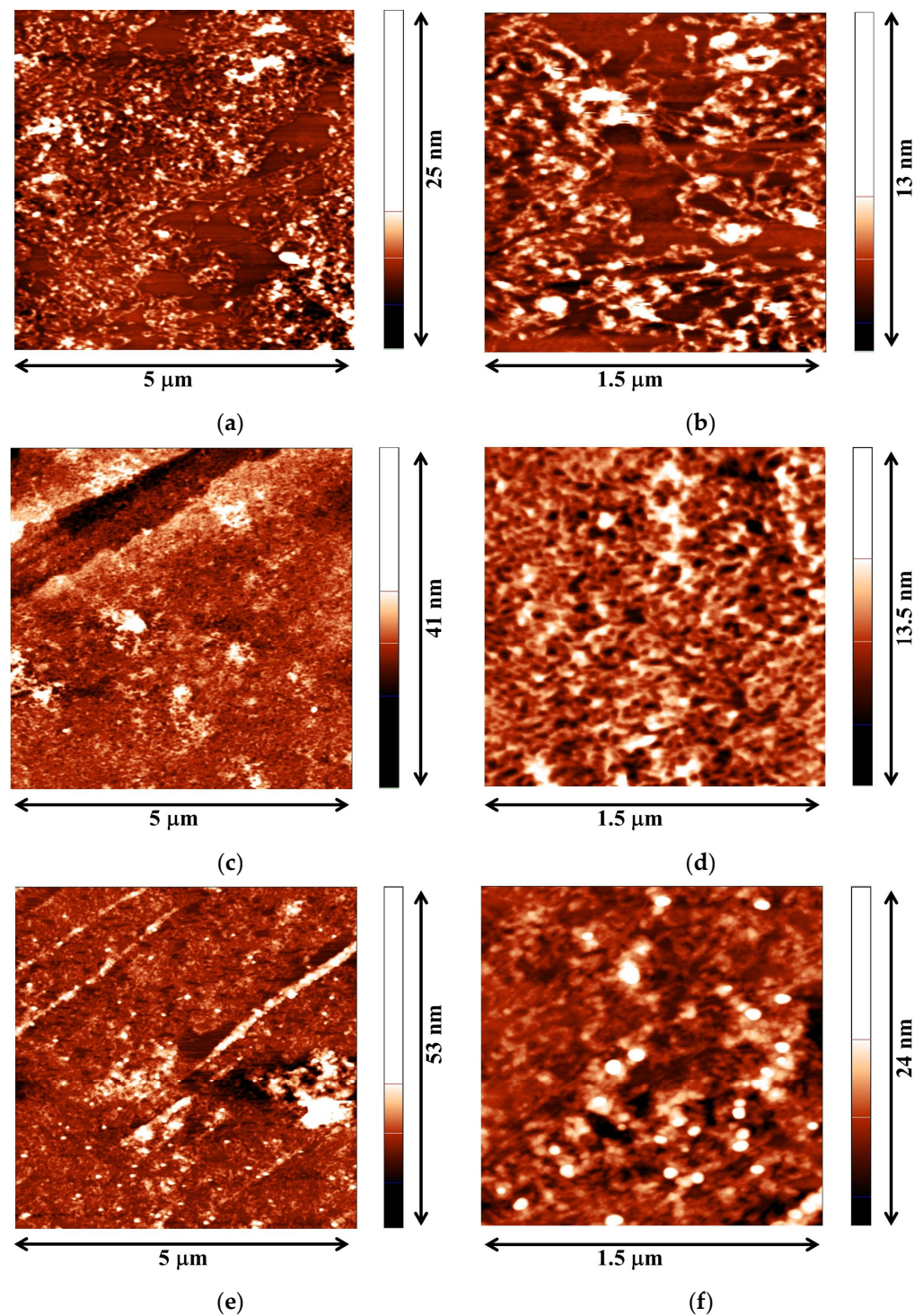


Figure 8. AFM images of spread layers of BSA fibrils at different degrees of surface compression: (a,b) before compression (surface pressure 4 mN/m); (c,d) twofold compression (surface pressure 22 mN/m); (e,f) fourfold compression (surface pressure 24 mN/m).

4. Conclusions

BSA fibrils form an almost continuous layer on the water surface, which cannot be destroyed by strong compressions and subsequent expansions. The layer is liquid-like and similar to that of the native protein but becomes more rigid upon surface compression. Unlike solutions of the native protein, the dispersions of BSA fibrils are characterized by an induction period of the kinetic dependencies of the dynamic surface elasticity and

surface tension and of slower changes of the surface properties as a result of significantly larger sizes of the fibrils as compared to the native protein molecules. The admixtures of polypeptides, which are formed during the fibril preparation and characterized by high surface activity, influence the surface properties of the fibril dispersions. The purification of the fibril dispersions leads to slower changes in the surface properties than for unpurified systems. The increase of the solution's ionic strength strongly accelerates the changes in the surface properties of dispersions of BSA fibrils, similar to lysozyme fibril dispersions [21], indicating a strong influence of electrostatic interactions in the layers of BSA fibrils. The properties of the spread layers of BSA fibrils differ from those of the fibril adsorption layers. This distinction can be caused by a slow propagation of the fibrils along the interface after spreading onto the liquid surface.

Supplementary Materials: The following supporting information can be downloaded at <https://www.mdpi.com/article/10.3390/colloids7030059/s1>, Figure S1: AFM-image of a droplet of fibril dispersions after dilution by 200 times in the TrisHCl buffer solution after purification; Figure S2: Compression–expansion isotherms of a spread layer of fibril dispersion on an aqueous solution of 0.1 M NaCl. Circles mark the places where the layer was transferred onto a mica plate; Figure S3: AFM images of spread layers of BSA fibrils transferred from the surface of a 0.1 M NaCl aqueous solution onto mica plates at the surface expansion to surface pressure of 10 mN/m; Figure S4: BAM-images of spread layers of BSA fibrils on the surface of 0.1 M NaCl aqueous solution at different degrees of surface compression-expansion: (a) before compression; (b) twofold compression; (c) twofold expansion after an external mechanical disturbance; (d) in ten minutes after the disturbance. Image size is 1×0.82 mm.

Author Contributions: Conceptualization, B.N.; methodology, B.N. and A.A.; formal analysis, G.L. and S.-Y.L.; investigation, G.L. and A.A.; writing-original draft preparation, A.A. and B.N.; writing-review and editing, B.N. and R.M.; supervision, R.M. All authors have read and agreed to the published version of the manuscript.

Funding: This research was funded by the RUSSIAN SCIENCE FOUNDATION, grant number 21-13-00039.

Data Availability Statement: Data are available upon reasonable request from the corresponding author.

Acknowledgments: The authors are grateful to the resource centers of SPbU (the Chemical Analysis and Materials Research Centre, Centre for Diagnostics of Functional Materials for Medicine, Pharmacology and Nanoelectronics, Interdisciplinary Resource Centre for Nanotechnology, Centre for Molecular and Cell Technologies) for the use of their equipment.

Conflicts of Interest: The authors declare no conflict of interest.

References

1. Dobson, C.M. Protein Misfolding, Evolution and Disease. *Trends Biochem. Sci.* **1999**, *24*, 329–332. [[CrossRef](#)] [[PubMed](#)]
2. Chiti, F.; Dobson, C.M. Protein Misfolding, Functional Amyloid, and Human Disease. *Annu. Rev. Biochem.* **2006**, *75*, 333–366. [[CrossRef](#)] [[PubMed](#)]
3. Eisenberg, D.; Jucker, M. The Amyloid State of Proteins in Human Diseases. *Cell* **2012**, *148*, 1188–1203. [[CrossRef](#)] [[PubMed](#)]
4. Dobson, C.M. The Amyloid Phenomenon and Its Links with Human Disease. *Cold Spring Harb. Perspect. Biol.* **2017**, *9*, a023648. [[CrossRef](#)] [[PubMed](#)]
5. Guo, J.; Arai, T.; Miklossy, J.; McGeer, P.L. A β and Tau Form Soluble Complexes That May Promote Self Aggregation of Both into the Insoluble Forms Observed in Alzheimer's Disease. *Proc. Natl. Acad. Sci. USA* **2005**, *103*, 1953–1958. [[CrossRef](#)] [[PubMed](#)]
6. Fowler, D.M.; Koulov, A.V.; Balch, W.E.; Kelly, J.W. Functional Amyloid—From Bacteria to Humans. *Trends Biochem. Sci.* **2007**, *32*, 217–224. [[CrossRef](#)] [[PubMed](#)]
7. Cao, Y.; Mezzenga, R. Food Protein Amyloid Fibrils: Origin, Structure, Formation, Characterization, Applications and Health Implications. *Adv. Colloid Interface Sci.* **2019**, *269*, 334–356. [[CrossRef](#)]
8. Knowles, T.P.J.; Mezzenga, R. Amyloid Fibrils as Building Blocks for Natural and Artificial Functional Materials. *Adv. Mater.* **2016**, *28*, 6546–6561. [[CrossRef](#)]
9. Wang, X.; Li, Y.; Zhong, C. Amyloid-Directed Assembly of Nanostructures and Functional Devices for Bionanoelectronics. *J. Mater. Chem. B* **2015**, *3*, 4953–4958. [[CrossRef](#)]
10. Manea, Y.K.; Khan, A.M.T.; Qashqoosh, M.; Wani, A.A.; Shahadat, M. Ciprofloxacin-Supported Chitosan/Polyphosphate Nanocomposite to Bind Bovine Serum Albumin: Its Application in Drug Delivery. *J. Mol. Liq.* **2019**, *292*, 111337. [[CrossRef](#)]

11. Sharma, V.; Kumar, A.; Ganguly, P.; Biradar, A.M.; Sharma, V.; Kumar, A.; Ganguly, P.; Biradar, A.M. Highly Sensitive Bovine Serum Albumin Biosensor Based on Liquid Crystal Highly Sensitive Bovine Serum Albumin Biosensor Based on Liquid Crystal. *Appl. Phys. Lett.* **2014**, *104*, 043705. [[CrossRef](#)]
12. Lai, Y.-R.; Wang, S.S.-S.; Hsu, T.-L.; Chou, S.-H.; How, S.-C.; Lin, T.-H. Application of Amyloid-Based Hybrid Membranes in Drug Delivery. *Polymers* **2023**, *15*, 1444. [[CrossRef](#)] [[PubMed](#)]
13. Mohammadian, M.; Madadlou, A. Technological Functionality and Biological Properties of Food Protein Nanofibrils Formed by Heating at Acidic Condition. *Trends Food Sci. Technol.* **2018**, *75*, 115–128. [[CrossRef](#)]
14. Li, C.; Qin, R.; Liu, R.; Miao, S.; Yang, P. Functional Amyloid Materials at Surfaces/Interfaces. *Biomater. Sci.* **2018**, *6*, 462–472. [[CrossRef](#)] [[PubMed](#)]
15. Wang, X.; Yue, C.; Xu, H.; Guan, C.; Guo, R.; Yang, X.; Ma, C.; Shao, M. Comparison of Emulsifying Properties of Fibrils Formed from Whey Protein Concentrate Following Induction by Nuclei and Nuclei Fragments. *Int. Dairy J.* **2021**, *123*, 105166. [[CrossRef](#)]
16. Fan, Y.; Peng, G.; Pang, X.; Wen, Z.; Yi, J. Physicochemical, Emulsifying, and Interfacial Properties of Different Whey Protein Aggregates Obtained by Thermal Treatment. *LWT* **2021**, *149*, 111904. [[CrossRef](#)]
17. Lam, S.; Velikov, K.P.; Velev, O.D. Pickering Stabilization of Foams and Emulsions with Particles of Biological Origin. *Curr. Opin. Colloid Interface Sci.* **2014**, *19*, 490–500. [[CrossRef](#)]
18. Sagis, L.M.C.; Humblet-Hua, K.N.P.; Kempen, S.E.H.J. van Nonlinear Stress Deformation Behavior of Interfaces Stabilized by Food-Based Ingredients. *J. Phys. Condens. Matter* **2014**, *26*, 464105. [[CrossRef](#)]
19. Humblet-Hua, N.P.K.; Van Der Linden, E.; Sagis, L.M.C. Surface Rheological Properties of Liquid-Liquid Interfaces Stabilized by Protein Fibrillar Aggregates and Protein-Polysaccharide Complexes. *Soft Matter* **2013**, *9*, 2154–2165. [[CrossRef](#)]
20. Ninham, B.W. The Loss of Certainty. In *Progress in Colloid and Polymer Science*; Springer: Berlin/Heidelberg, Germany, 2002; Volume 120, pp. 1–12.
21. Noskov, B.A.; Akentiev, A.V.; Bykov, A.G.; Loglio, G.; Miller, R.; Milyaeva, O.Y. Spread and Adsorbed Layers of Protein Fibrils at Water–Air Interface. *Colloids Surf. B Biointerfaces* **2022**, *220*, 112942. [[CrossRef](#)]
22. Jordens, S.; Ru, P.A.; Sieber, C.; Isa, L.; Fischer, P.; Mezzenga, R. Bridging the Gap between the Nanostructural Organization and Macroscopic Interfacial Rheology of Amyloid Fibrils at Liquid Interfaces. *Langmuir* **2014**, *30*, 10090–10097. [[CrossRef](#)]
23. Rühls, P.A.A.; Scheuble, N.; Windhab, E.J.J.; Fischer, P. Protein Adsorption and Interfacial Rheology Interfering in Dilatational Experiment. *Eur. Phys. J. Spec. Top.* **2013**, *222*, 47. [[CrossRef](#)]
24. Jordens, S.; Riley, E.E.; Usov, I.; Isa, L.; Olmsted, P.D.; Mezzenga, R. Adsorption at Liquid Interfaces Induces Amyloid Fibril Bending and Ring Formation. *ACS Nano* **2014**, *8*, 11071–11079. [[CrossRef](#)] [[PubMed](#)]
25. Wang, H.; Gong, Y.; Lu, W.; Chen, B. Influence of Nano-SiO₂ on Dilational Viscoelasticity of Liquid/Air Interface of Cetyltrimethyl Ammonium Bromide. *Appl. Surf. Sci.* **2008**, *254*, 3380–3384. [[CrossRef](#)]
26. Ghadami, S.A.; Ahmadi, Z.; Moosavi-Nejad, Z. The Albumin-Based Nanoparticle Formation in Relation to Protein Aggregation. *Spectrochim. Acta—Part A Mol. Biomol. Spectrosc.* **2021**, *252*, 119489. [[CrossRef](#)] [[PubMed](#)]
27. Holm, N.K.; Jespersen, S.K.; Thomassen, L.V.; Wolff, T.Y.; Sehgal, P.; Thomsen, L.A.; Christiansen, G.; Andersen, C.B.; Knudsen, A.D.; Otzen, D.E. Aggregation and Fibrillation of Bovine Serum Albumin. *Biochim. Biophys. Acta—Proteins Proteom.* **2007**, *1774*, 1128–1138. [[CrossRef](#)] [[PubMed](#)]
28. Jordens, S.; Isa, L.; Usov, I.; Mezzenga, R. Non-Equilibrium Nature of Two-Dimensional Isotropic and Nematic Coexistence in Amyloid Fibrils at Liquid Interfaces. *Nat. Commun.* **2013**, *4*, 1917–1918. [[CrossRef](#)]
29. Usov, I.; Adamcik, J.; Mezzenga, R. Polymorphism Complexity and Handedness Inversion in Serum Albumin Amyloid Fibrils. *ACS Nano* **2013**, *7*, 10465–10474. [[CrossRef](#)]
30. Usov, I.; Adamcik, J.; Mezzenga, R. Polymorphism in Bovine Serum Albumin Fibrils: Morphology and Statistical Analysis. *Faraday Discuss.* **2013**, *166*, 151–162. [[CrossRef](#)]
31. Dahal, E.; Choi, M.; Alam, N.; Bhirde, A.A.; Beaucage, S.L.; Badano, A. Structural Evaluation of an Amyloid Fibril Model Using Small-Angle X-ray Scattering. *Phys. Biol.* **2017**, *14*, 046001. [[CrossRef](#)]
32. Lambrecht, M.A.; Jansens, K.J.A.; Rombouts, I.; Brijs, K.; Rousseau, F.; Schymkowitz, J.; Delcour, J.A. Conditions Governing Food Protein Amyloid Fibril Formation. Part II: Milk and Legume Proteins. *Compr. Rev. Food Sci. Food Saf.* **2019**, *18*, 1277–1291. [[CrossRef](#)] [[PubMed](#)]
33. Bhattacharya, M.; Jain, N.; Mukhopadhyay, S. Insights into the Mechanism of Aggregation and Fibril Formation from Bovine Serum Albumin. *J. Phys. Chem. B* **2011**, *115*, 4195–4205. [[CrossRef](#)] [[PubMed](#)]
34. Nirwal, S.; Bharathi, V.; Patel, B.K. Amyloid-like Aggregation of Bovine Serum Albumin at Physiological Temperature Induced by Cross-Seeding Effect of HEWL Amyloid Aggregates. *Biophys. Chem.* **2021**, *278*, 106678. [[CrossRef](#)] [[PubMed](#)]
35. Yaseen, Z.; Rehman, S.U.; Tabish, M.; Shalla, A.H.; Kabir-ud-Din, K.-D. Modulation of Bovine Serum Albumin Fibrillation by Ester Bonded and Conventional Gemini Surfactants. *RSC Adv.* **2015**, *5*, 58616–58624. [[CrossRef](#)]
36. Veerman, C.; Sagis, L.M.C.; Heck, J.; Van Der Linden, E. Mesostructure of Fibrillar Bovine Serum Albumin Gels. *Int. J. Biol. Macromol.* **2003**, *31*, 139–146. [[CrossRef](#)] [[PubMed](#)]
37. Jung, J.; Gunes, D.Z.; Mezzenga, R. Interfacial Activity and Interfacial Shear Rheology of Native β -Lactoglobulin Monomers and Their Heat-Induced Fibers. *Langmuir* **2010**, *26*, 15366–15375. [[CrossRef](#)] [[PubMed](#)]
38. Wan, Z.; Yang, X.; Sagis, L.M.C. Contribution of Long Fibrils and Peptides to Surface and Foaming Behavior of Soy Protein Fibril System. *Langmuir* **2016**, *32*, 8092–8101. [[CrossRef](#)] [[PubMed](#)]

39. Noskov, B.A.; Akentiev, A.V.; Bilibin, A.Y.; Zorin, I.M.; Miller, R. Dilational Surface Viscoelasticity of Polymer Solutions. *Adv. Colloid Interface Sci.* **2003**, *104*, 245–271. [[CrossRef](#)]
40. Noskov, B.A.; Isakov, N.A.; Gochev, G.; Loglio, G.; Miller, R. Interaction of Fullerene C60 with Bovine Serum Albumin at the Water–Air Interface. *Colloids Surf. A Physicochem. Eng. Asp.* **2021**, *631*, 127702. [[CrossRef](#)]
41. Noskov, B.; Mikhailovskaya, A. Adsorption Kinetics of Globular Proteins and Protein/Surfactant Complexes at the Liquid–Gas Interface. *Soft Matter* **2013**, *9*, 9392–9402. [[CrossRef](#)]
42. Karaman, M.E.; Ninham, B.W.; Pashley, R.M. Effects of Dissolved Gas on Emulsions, Emulsion Polymerization, and Surfactant Aggregation. *J. Phys. Chem.* **1996**, *100*, 15503–15507. [[CrossRef](#)]
43. Milyaeva, O.Y.; Akentiev, A.V.; Bykov, A.G.; Lin, S.; Loglio, G.; Miller, R.; Michailov, A.V.; Rotanova, K.Y.; Noskov, B.A. Spread Layers of Lysozyme Microgel at Liquid Surface. *Polymers* **2022**, *14*, 3979. [[CrossRef](#)]

Disclaimer/Publisher’s Note: The statements, opinions and data contained in all publications are solely those of the individual author(s) and contributor(s) and not of MDPI and/or the editor(s). MDPI and/or the editor(s) disclaim responsibility for any injury to people or property resulting from any ideas, methods, instructions or products referred to in the content.